

# Modelling topographic effects in GOCE gravity gradients

Grombein T., Seitz K., Heck B.

Geodetic Institute, Karlsruhe Institute of Technology (KIT), Englerstraße 7, D-76128 Karlsruhe, Germany,

E-Mail: thomas.grombein@kit.edu

## 1. Introduction

The basic observables of the satellite gravity gradiometry mission GOCE (Gravity Field and Steady-State Ocean Circulation Explorer) are the second-order derivatives of the Earth's gravitational potential  $V$  (components of the symmetric Marussi tensor  $\mathbf{M}$ ). These gravity gradients can be defined in a local north oriented frame (LNOF) whose x-axis is pointing North, y-axis towards West and z-axis upwards in geocentric radial direction:

$$\mathbf{M} = \vec{\nabla} (\vec{\nabla} V) = \begin{bmatrix} V_{11} & V_{12} & V_{13} \\ V_{12} & V_{22} & V_{23} \\ V_{13} & V_{23} & V_{33} \end{bmatrix} = \begin{bmatrix} V_{xx} & V_{xy} & V_{xz} \\ V_{xy} & V_{yy} & V_{yz} \\ V_{xz} & V_{yz} & V_{zz} \end{bmatrix}.$$

Gravity gradients observed by GOCE contain significant high- and mid-frequency components resulting from the attraction of the topographic (and isostatic) masses of the Earth. The existence of these signal components with short-wavelength affects the further processing of GOCE observation data, e.g. in the framework of regional and global gravity field modelling or the combination with terrestrial gravity anomalies. In all of these applications the harmonic downward continuation of the observed gradients from satellite height to mean sea level (MSL) can be seen as an ill-conditioned process. In order to mitigate the instability of downward continuation, it is recommended to smooth the gradients by applying topographic and isostatic reductions (*Wild-Pfeiffer, 2007, 2008*). In work package (WP) 150 of the REAL GOCE project the focus is laid on the efficient numerical modelling and calculation of topographic and isostatic effects in the observed GOCE gravity gradients.

In this paper we will concentrate on modelling topographic effects. In the first part we describe how to model them and discuss the input data and different modelling parameters. To quantify the influence of these parameters several numerical tests have been performed, which are presented and analyzed in the second part. Based on these results we try to figure out the »best fitting« modelling parameters for an efficient calculation of topographic effects in the context of the GOCE satellite mission.

## 2. Modelling topographic effects

The modelling of topographic effects in gravity gradients as observed by GOCE is based on the numerical evaluation of functionals of Newton's integral extending over the domain of the topographic masses which include the masses of the continents as well as the oceanic masses. In order to evaluate these kinds of volume integrals, the geometry of the topographic boundary surface and the density function inside the topographic masses must be known. Due to the fact that the topography is only known at discrete points (represented by a digital terrain model (DTM) with a specific grid resolution) it is not possible to evaluate Newton's integral directly over the entire domain. Practical numerical computations rely on a discretization and approximation of the problem. The topographic masses are usually decomposed into regular elementary bodies, where their density is assumed to be constant. Newton's integral is then evaluated for each particular body and the total effect is calculated by summation. For the decomposition,

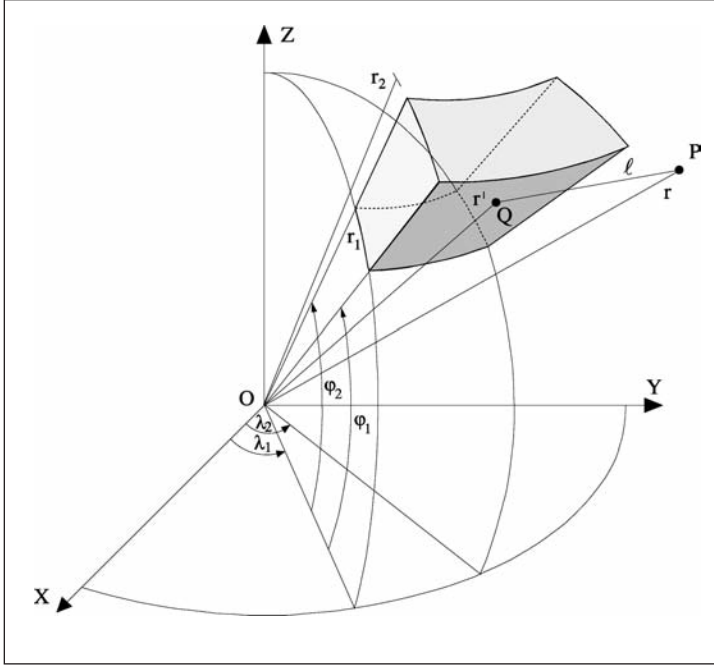


Figure 1: Geometry of a tesseroid (Kuhn, 2000)

various geometric elementary bodies such as tesseroids, prisms or point-masses can be used. Tesseroids are bodies bounded by three pairs of surfaces: A pair of concentric spheres ( $r_1 = \text{const}$ ,  $r_2 = \text{const}$ ), a pair of meridional planes ( $\lambda_1 = \text{const}$ ,  $\lambda_2 = \text{const}$ ) and a pair of coaxial circular cones defined by the parallels  $\varphi_1 = \text{const}$ ,  $\varphi_2 = \text{const}$  (Fig. 1, cf. Heck and Seitz, 2007). Tesseroids are well suited for the decomposition if the topography of the Earth is represented by a DTM which is usually given in geographical coordinates. Based on Newton's integral the effect of a tesseroid on gravity gradients can be determined by optimized, non-singular tesseroid formulas (cf. Grombein et al., 2010a):

$$V_{ij} = G\rho \int_{\lambda_1}^{\lambda_2} \int_{\varphi_1}^{\varphi_2} \int_{r_1}^{r_2} \left( \frac{3\Delta x_i \Delta x_j}{\ell^5} - \frac{\delta_{ij}}{\ell^3} \right) r'^2 \cos \varphi' dr' d\varphi' d\lambda'$$

$$i, j \in \{1, 2, 3\}$$

$$\Delta x_1 = r' \cos \varphi \sin \varphi' - \sin \varphi \cos \varphi' \cos (\lambda' - \lambda)$$

$$\Delta x_2 = -r' \cos \varphi \sin (\lambda' - \lambda)$$

$$\Delta x_3 = r' \cos \psi - r.$$

In these formulas  $G$  denotes Newton's gravitational constant and  $\rho$  the constant density value of the tesseroid. The Euclidean distance between the computation point  $P(r, \varphi, \lambda)$  and the running integration point  $Q(r', \varphi', \lambda')$  is denoted by  $\ell$ . Since the respective volume integrals for tesseroids cannot be solved analy-

tically, numerical methods have to be applied, which will be described below.

### 3. Input data and modelling parameters

In Fig. 2 an overview of the required input data and the parameters for the modelling of topographic effects is given. The most important input data is global information about topography and density. As mentioned above, precise models of Earth's topography are available through global high-resolution DTMs. Compared to this high-resolution topography information, global density models only exist in a very low resolution, like the Crust2.0 model of seismic velocities and density (Bassin et al., 2000; Tsoulis, 2004). Therefore, regarding density, assumptions for the modelling of topographic effects have to be made. If there is no further information, topographic masses respectively the particular tesseroids are usually modelled with a standard density value of  $\rho = 2670 \text{ kg/m}^3$ , which represents an average of rock density at the Earth's surface. Since this is only a very rough approximation, it is better to use at least combined topography/bathymetry models such as SRTM30\_PLUS (Becker et al., 2009), allowing to model the ocean masses with a corresponding density value, additionally. Another class of DTMs, which will be used in our research, are global topographic databases



Figure 2: Input data and modelling parameters for the calculation of topographic effects

like DTM2006.0 (Pavlis et al., 2007), which was developed for compiling the Earth Gravitation Model EGM2008, or the former JGP95E (Lemoine et al., 1998). Beside topographic heights and bathymetric depths these DTMs also contain further details about ice thickness and lake depths. Each grid element is classified by six terrain types: (1) Dry Land Below MSL, (2) Lake, (3) Oceanic Ice Shelf, (4) Ocean, (5) Grounded Glacier, (6) Dry Land Above MSL.

A common way to take different density values of terrain types into account is the concept of rock-equivalent heights (Kuhn and Seitz, 2005; Rummel et al., 1988). Based on the principle of mass balance the DTM heights of different terrain types are converted into rock-equivalent heights with respect to a constant reference density (e.g.  $\rho = 2670 \text{ kg/m}^3$ ). Corresponding formulas for a spherical approximation are explicitly given in Kuhn and Seitz (2005). The use of this method allows a simple modelling of different terrain types with only one density value which also means that for each grid element the effect of only one tesseroid has to be calculated. The disadvantage of this approach is that the geometry of the mass distribution changes if the actual mass-density is strongly different from the adopted constant density value (Tsoulis and Kuhn, 2007). To avoid this effect a rigorous, separate modelling of different terrain types in a vertical arrangement is necessary. As a consequence, the computation

time for the whole calculation process is increasing. Within our developed Rock-Water-Ice method (RWI method) the database of the 5' x 5' DTM2006.0 is used to compile a three layer model, where each grid element consists of a rock, water and ice proportion in vertical direction. Consequently, for each grid element the topographic masses are modelled by three tesseroids with different heights of the respective top surface ( $h_R, h_W, h_I$ ) in relation to MSL and consistent thickness ( $t_R, t_W, t_I$ ) and density values ( $\rho_R = 2760 \text{ kg/m}^3, \rho_W = 1000 \text{ kg/m}^3, \rho_I = 920 \text{ kg/m}^3$ ), see Fig. 3.

Beside the topographic and density information which define the geometry and mass of the particular tesseroids, their spatial arrangement has to be fixed. Even though the used tesseroid formulas are given in a spherical manner, these bodies can be set up on different reference surfaces approximating MSL. We can either arrange them on a spherical earth of constant mean radius or, in a more realistic composition, on the surface of an ellipsoid of revolution. Through the different arrangement of the topography the distance between an arbitrary computation point and the tesseroid bodies changes and therefore affects the impact on the gravity gradients.

When the tesseroids are defined in size and fixed in space, we have to constitute, how to evaluate the volume integrals of the tesseroid

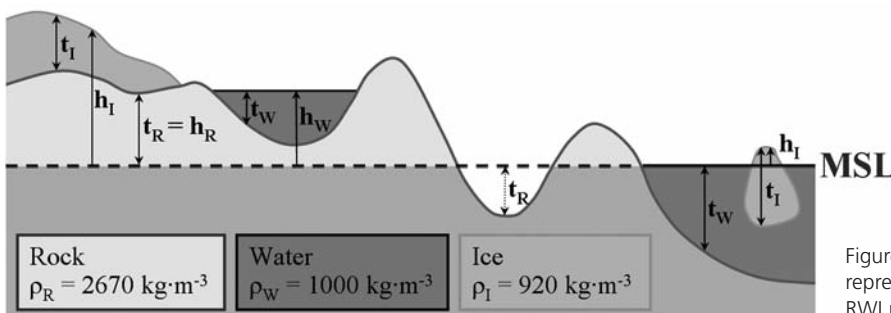


Figure 3: Schematic representation of the RWI method

formulas. As mentioned above, there is no analytical solution due to occurring elliptical integrals. Therefore, another modelling parameter is the calculation method used for solving these volume integrals numerically with a specific approximation quality. A second-order approximation has been developed at the Geodetic Institute Karlsruhe and proposed by *Heck and Seitz (2007)*. This approach is based on a Taylor series expansion of the integral kernel and subsequent term-wise integration. It can be seen as an extension of MacMillan's approximation for the prism formulas (*MacMillan, 1930*). While *Heck and Seitz (2007)* originally consider the effect on the potential and on gravity, in *Wild-Pfeiffer (2007, 2008)* this approach is extended on gravity gradients. As an alternative to Taylor series expansions, Gauss-Legendre cubature (3D) has been investigated by *Wild-Pfeiffer (2007, 2008)*. Depending on the number of used nodes Gauss-Legendre cubature (3D) reaches a higher approximation quality than Taylor series expansion, but on the other hand more computation time is required. Since the effect of distant masses on functionals of the gravitational potential diminishes, for remote bodies a tesseroid can also be approximated by a point-mass, which concentrates the whole mass of the tesseroid to its geometric centre. For a more detailed description of the mentioned calculation procedures as well as the explicit numerical calculation formulas related to the presented optimized tesseroid formulas see *Grombein et al. (2010a)*. It should be mentioned that the accuracy which is achievable with a specific calculation method also depends on the DTM resolution and thus on the level of decomposition of the topographic masses.

#### 4. Numerical Investigations

In order to quantify the impact of the discussed parameters, several numerical tests have been performed, where topographic effects in gravity gradients were calculated on a grid in the satellite height of GOCE. The computation points are located on a GOCE-like circular orbit with a geocentric radius  $r = R + h$ . The mean

earth radius is  $R = 6378.137$  km and  $h = 254.9$  km is the adopted altitude of GOCE. For the analysis differences between any two options were performed, where only one modelling parameter was varied in order to avoid interfering effects. The differences in the gravity gradients are plotted for the  $V_{zz}$  component and are described by statistical parameters for all components. In order to find an efficient method of calculation by analyzing the modelling parameters, it is necessary to obtain a good balance between achievable accuracy and required computation time. In our application the accuracy of the topographic effects should be adjusted with the measuring accuracy of the GOCE gravity gradients (1-2 mE). Therefore, an adequate level of accuracy (LOA) seems to be  $\pm 10^{-2}$  mE. Remind that the absolute topographic effects in gravity gradients observed in the satellite height of GOCE are in the range of about  $\pm 8$  E (*Wild-Pfeiffer 2007, 2008*).

#### Digital Terrain Model

Calculations with the 5' x 5' DTM2006.0 as well as with the 5' x 5' JGP95E have been performed. The differences in the gravity gradients are in the range of -964 to 1319 mE (Tab. 1) and therefore far beyond the defined LOA. As can be seen in Fig. 4 the maximum and minimum differences are located in Antarctica and the northern part of Greenland, i.e. in regions with large ice masses. On the one hand, this discrepancy might be explained with a mass displacement and melting of the ice masses within the long time period between the creation of the DTM2006.0 and the JGP95E. On the other hand, when comparing both DTMs it becomes apparent that in these regions much more high-resolution input data were included in the DTM2006.0. Since the DTM2006.0 was generally generated by actual data and especially by much more high-resolution sources this DTM will be preferred. However, this comparison clearly illustrates that the differences induced by different DTMs can cause very large effects, and thus raises the question which DTM reflects best the »real« topography of the Earth.

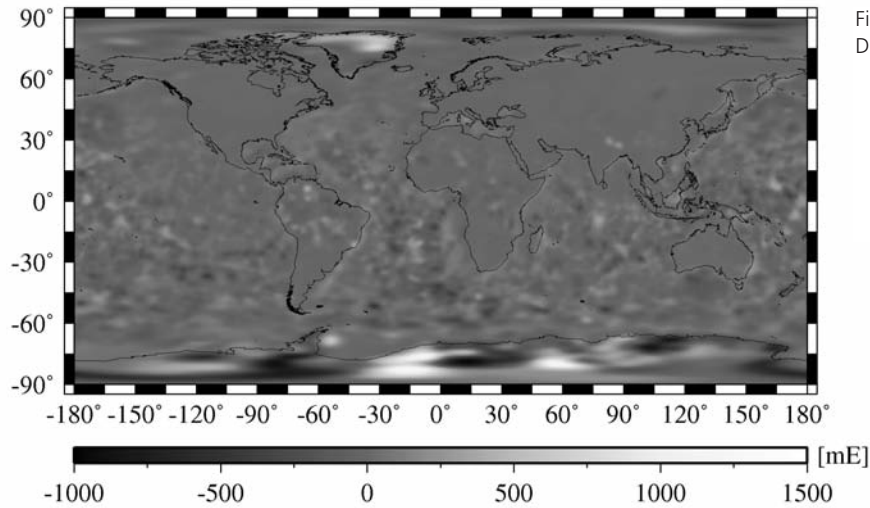


Figure 4:  $V_{zz}$  differences: Digital Terrain Model

Table 1: Statistics: Digital Terrain Model in [mE]

	$V_{xx}$	$V_{xy}$	$V_{xz}$	$V_{yy}$	$V_{yz}$	$V_{zz}$
<b>min</b>	-528.724	-347.615	-542.222	-956.719	-945.074	-964.381
<b>max</b>	567.424	327.154	649.586	686.143	981.729	1319.323
<b>mean</b>	2.047	0.000	-2.568	4.421	0.000	-6.467
<b>rms</b>	70.083	42.868	82.321	87.804	105.659	130.788

### Density

The discussed density concepts of rock-equivalent heights and the RWI method are compared based on the information of the DTM2006.0 database. Tab. 2 describes the statistics of the differences: The minimum is reached in the  $V_{zz}$  component and has a value of -19 mE; the maximum can be found in the  $V_{yz}$  component and amounts to 24 mE. The illustration in Fig. 5 shows that the differences can be classified according to the three areas: rock, water and ice. In the case of the continental rock areas the differences are zero due to the fact that in both approaches the modelling is the same. Although the density contrast between rock and ice is the most extreme, the differences for the ice areas are also relatively small. The largest differences can be registered in the case of water areas, especially at the sites of deep ocean trenches or mid-ocean ridges, like the Mid-Atlantic ridge. Therefore, the mass displacement in the concept of rock-equivalent heights is not only influenced by large density contrasts between the constant

and actual density value, but also by the magnitude of the condensed height itself. Since the differences show that the resulting effects also exceed the defined LOA, it is proposed to use the more realistic but also more time consuming RWI method.

### Mass arrangement

To investigate the impact of the mass arrangement, tesseroids have been set up on a spherical earth of constant radius  $R = 6378.137$  km as well as on the surface of an ellipsoid of revolution (GRS80; Moritz, 1980). In both cases the GOCE orbit is still assumed circular. The differences in the modelled topographic effects between the spherical and ellipsoidal arrangement of the topography are in a range of -268 to 336 mE (see Tab 3.). The minimum value is reached in the  $V_{xz}$  component, the maximum in the  $V_{zz}$  component. In general, the differences are minimum near the equator and increase towards the polar regions (see Fig. 6). This trend clearly illustrates that the differences originate from the earth flattening which effects



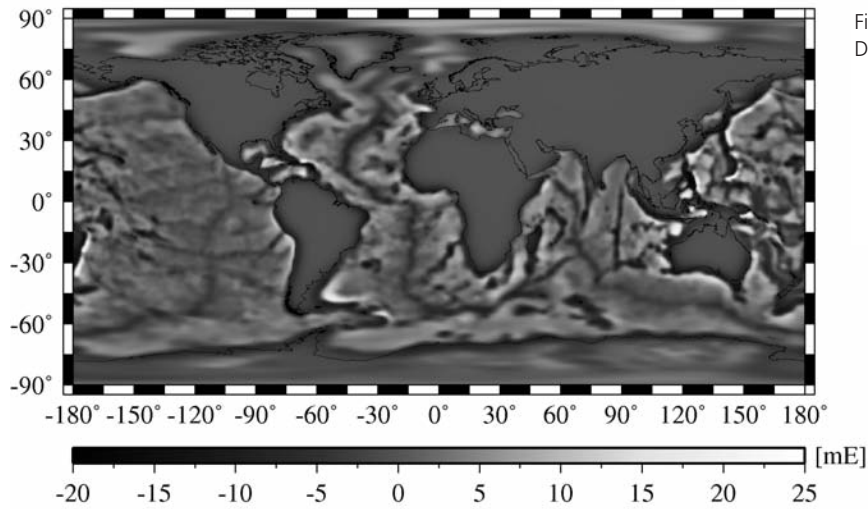


Figure 5:  $V_{zz}$  differences:  
Density

Table 2: Statistics: Density in [mE]

	$V_{xx}$	$V_{xy}$	$V_{xz}$	$V_{yy}$	$V_{yz}$	$V_{zz}$
<b>min</b>	-17.262	-9.497	-18.694	-16.105	-16.144	-18.919
<b>max</b>	13.813	7.322	17.406	16.660	24.419	21.296
<b>mean</b>	0.054	0.000	-0.072	-0.016	0.000	-0.038
<b>rms</b>	2.132	1.111	2.451	2.040	2.360	3.472

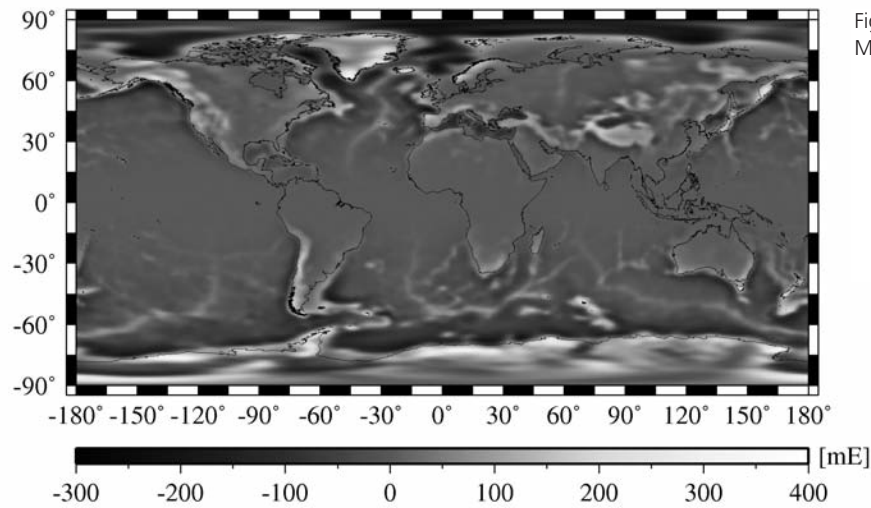


Figure 6:  $V_{zz}$  differences:  
Mass arrangement

Table 3: Statistics: Mass arrangement in [mE]

	$V_{xx}$	$V_{xy}$	$V_{xz}$	$V_{yy}$	$V_{yz}$	$V_{zz}$
<b>min</b>	-235.192	-91.489	-268.123	-216.036	-220.136	-258.573
<b>max</b>	186.915	104.707	276.636	227.854	226.204	336.387
<b>mean</b>	0.253	0.000	5.873	0.778	0.000	-1.031
<b>rms</b>	38.451	17.880	43.943	33.740	37.084	60.551

a mass displacement particularly in the polar regions. In many applications spherical approximation yields sufficient results, but in this study the differences reach an order of magnitude above the defined LOA. The ellipticity of the reference surface cannot be neglected and should be considered when modelling topographic effects in gravity gradients for a satellite-mission like GOCE (cf. *Grombein et al., 2010b*).

**Calculation method**

Finally, the use of different calculation methods for the solution of the tesseroïd formulas has to be investigated. Previous investigations (*Grombein et. al, 2010a*) have already theoretically shown that the Gauss-Legendre cubature (3D) with 27 nodes in combination with a DTM resolution of 5' x 5' will guarantee the defined LOA, if the computation point P is situated in satellite height. In the numerical tests performed in the present study with the use of the 5' x 5' DTM2006.0 it was found that calcu-

lations with Taylor series expansions and Gauss-Legendre cubature (3D) with 8 as well as with 27 nodes provide the same results within the defined LOA. The differences between the use of Taylor series expansions and the much faster point-mass approximation are shown in Fig. 7 and are described by the statistics in Tab. 4. It can be realized that the differences are strongly correlated with the topography. The minimum values (about -0.7 mE) are reached over large mountain ranges such as the Andes or the Himalaya. The maximum values (about 0.8 mE) can be found at the continental boundaries. Since the differences are an order of magnitude above the defined LOA, the Taylor series expansion cannot be replaced by the point-mass approximation.

To reduce the computation time it seems beneficial to use a combination of the Taylor series expansion and the point-mass approximation. A common approach for a combination is to divide the total integration area into a near

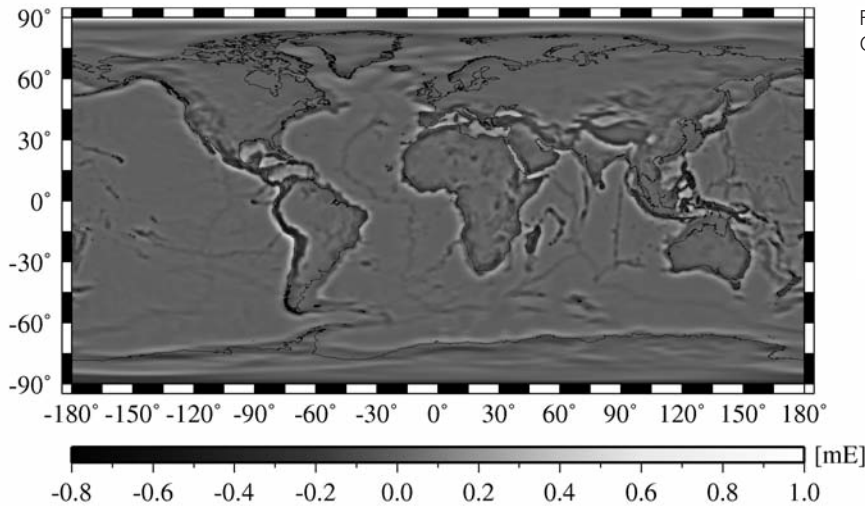


Figure 7:  $V_{zz}$  differences: Calculation method

Table 4: Statistics: Calculation method in [mE]

	$V_{xx}$	$V_{xy}$	$V_{xz}$	$V_{yy}$	$V_{yz}$	$V_{zz}$
<b>min</b>	-0.413	-0.323	-0.474	-0.424	-0.536	-0.739
<b>max</b>	0.475	0.270	0.652	0.542	0.476	0.824
<b>mean</b>	0.000	0.000	-0.009	-0.003	0.000	0.003
<b>rms</b>	0.054	0.022	0.063	0.053	0.041	0.093

and far zone with respect to the spherical distance from the computation point. The near zone of the computation point is then modelled with the more accurate but slower Taylor series expansion, while the diminishing influence of the remote masses of the far zone are modelled with the much faster point-mass approximation. To apply such an approach a value for the spherical distance  $\Psi_c$  which defines the boundary between the near and far zone has to be fixed. In Fig. 8 the maximum (absolute) difference that occurs in an arbitrary computation point between the results of the Taylor series expansion and the combined approach is plotted in relation to spherical distance values in a logarithmic scale. The resulting curve shows that the differences increase almost exponentially when the spherical distance is decreasing. In order to guarantee the LOA the spherical distance should not be smaller than  $\Psi_c = 11^\circ$ .

## 5. Conclusions and Outlook

In this paper the modelling process of topographic effects in gravity gradients was described and the handling of several modelling parameters was discussed. With the help of numerical tests the impact of these parameters on gravity gradients could be quantified. In the context of the GOCE satellite mission and relating to the measuring accuracy of the obser-

ved gradients suitable modelling parameters have been proposed to get an efficient calculation method regarding computation time and accuracy.

As input data the global topographic database of the 5' x 5' DTM2006.0 is used for the description of the topographic surface as well as for providing information about the density, which is modelled with the RWI method. According to the DTM resolution the topographic masses are decomposed into tesseroids which are arranged on an ellipsoidal reference surface. For the numerical solution of the tesseroid formulas the Taylor series expansion is used in the near zone of the computation point whereas in the far zone (beginning at a spherical distance of  $\Psi_c = 11^\circ$ ) a point-mass approximation is applied.

In the next step, the selected parameters will be used to model topographic effects in real GOCE observations of gravity gradients as well as to determine the isostatic signal components that were not discussed in this paper. Furthermore, the degree of smoothing of the gradients after applying the combined topographic-isostatic reductions will be investigated and compared to other possible smoothing approaches.

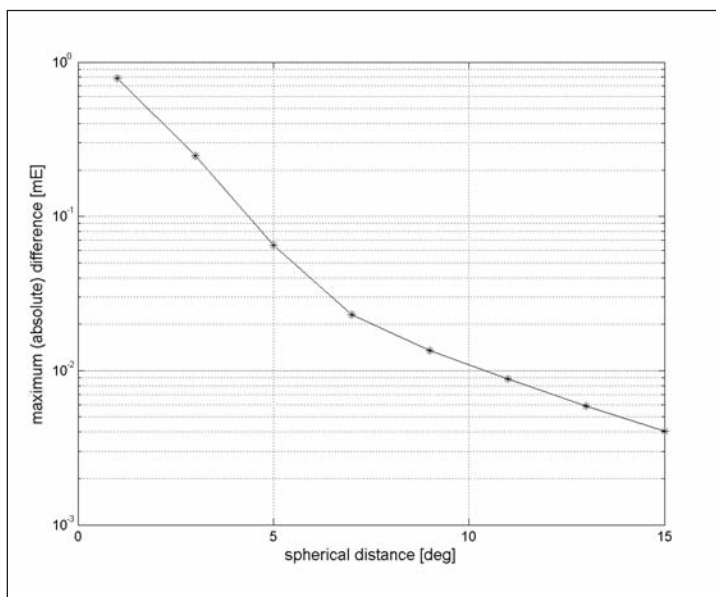


Figure 8: Defining the near and far zone



## Acknowledgements

The authors would like to thank N.K. Pavlis for providing the Global Digital Terrain Model DTM2006.0. The Bundesministerium für Bildung und Forschung (BMBF, German Federal Ministry of Education and Research) is acknowledged for the financial support of this research within the REAL GOCE project of the GEOTECHNOLOGIEN Programme.

## References

- Bassin C., Laske G., Masters G. (2000): The current limits of resolution for surface wave tomography in North America. *EOS Trans AGU* 81 (48), F897.
- Becker J.J., Sandwell D.T., Smith W.H.F., Braud J., Binder B., Depner J., Fabre D., Factor J., Ingalls S., Kim S-H., Ladner R., Marks K., Nelson S., Pharaoh A., Trimmer R., von Rosenberg J., Wallace G., Weatherall P. (2009): Global Bathymetry and Elevation Data at 30 Arc Seconds Resolution: SRTM30\_PLUS. *Marine Geodesy*, 32(4):355-371.
- Grombein T., Seitz K., Heck B. (2010a): Untersuchungen zur effizienten Berechnung topographischer Effekte auf den Gradiententensor am Fallbeispiel der Satellitengradiometriemission GOCE. KIT Scientific Reports 7547, Schriftenreihe des Studiengangs Geodäsie und Geoinformatik, No. 2010/1, KIT Scientific Publishing, Karlsruhe.
- Grombein T., Seitz K., Heck B. (2010b): Spherical and ellipsoidal arrangement of the topography and its impact on gravity gradients in the GOCE mission. Presented at the General Assembly of the European Geosciences Union, Vienna, Austria, 2-7 May 2010.
- Heck B., Seitz K. (2007): A comparison of the tesseroid, prism and point-mass approaches for mass reductions in gravity field modelling. *JGeod*, 81(2):121–136, DOI: 10.1007/s00190-006-0094-0.
- Kuhn M. (2000): Geoidbestimmung unter Verwendung verschiedener Dichtehypothesen. Deutsche Geodätische Kommission, C520, München.
- Kuhn M., Seitz K. (2005): Comparison of Newton's integral in the space and frequency domains. In: Sansò F. (ed.): *A Window on the Future of Geodesy*. IAG Symposia Vol. 128, Springer, 386-391.
- Lemoine F.G., Kenyon S.C., Factor J.K., Trimmer R.G., Pavlis N.K., Chinn D.S., Cox C.M., Klosko S.M., Luthcke S.B., Torrence M.H., Wang Y.M., Williamson R.G., Pavlis E.C., Rapp R.H., Olson T.R. (1998): The Development of the Joint NASA GSFC and the National Imagery and Mapping Agency (NIMA) Geopotential Model EGM96. NASA Goddard Space Flight Center, Greenbelt, Maryland, USA.
- MacMillan W.D. (1930): *Theoretical Mechanics*, Vol 2: the Theory of the potential. McGraw-Hill, New York (reprinted by Dover Publications, New York, 1958).
- Moritz, H. (1980): Geodetic reference system 1980. *Bulletin Géodésique*, 54:395–405.
- Pavlis N.K., Factor J.K., Holmes S.A. (2007): Terrain-related gravimetric quantities computed for the next EGM. In: Kiliçoglu A., Forsberg R. (eds.): *Gravity Field of the Earth*, Proceedings of the 1st International Symposium of the IGFS, Istanbul, Turkey, 318-323.
- Rummel R., Rapp H.R., Sünkel H., Tscherning C.C. (1988): Comparison of global topographic/isostatic models to the Earth's observed gravity field, Report No. 388, Department of Geodeic Science and Surveying, The Ohio State University, Columbus, 33 pp.
- Tsouli D. (2004): Spherical harmonic analysis of the CRUST 2.0 global crustal model. *JGeod*, 78 (1-2):7-11, DOI: 10.1007/s00190-003-0360-3.

Tsoulis D., Kuhn M. (2007): Recent developments in synthetic Earth gravity models in view of the availability of digital terrain and crustal databases of global coverage and increased resolution. In: Kiliçoglu A., Forsberg R. (eds.): Gravity Field of the Earth, Proceedings of the 1st International Symposium of the IGFS, Istanbul, Turkey, 354–359.

Wild-Pfeiffer F. (2007): Auswirkungen topographisch-isostatischer Massen auf die Satellitengradiometrie. Deutsche Geodätische Kommission, C604, München.

Wild-Pfeiffer, F. (2008): A comparison of different mass elements for use in gravity gradiometry. *JGeod*, 82(10):637-653, DOI: 10.1007/s00190-008-0219-8.